31st Congress of the International Council of the Aeronautical Sciences

Belo Horizonte, Brazil; September 09-14, 2018

ACTUATOR AND SENSOR PLACEMENT FOR CLOSED-LOOP CONTROL OF CONVECTIVE INSTABILITIES

Guilherme A. Freire* , **André V. G. Cavalieri*** , **Flávio J. Silvestre***

***Instituto Tecnológico de Aeronáutica, São José dos Campos, SP, 12228-900, Brazil**

Keywords: *Convective instabilities, Closed-loop control*

Abstract

This work deals with the characterization of the control of convective wavepackets, typical of the initial stages of transition to turbulence, using the Kuramoto-Sivashinsky equation [1] as a model problem representative of the transitional 2D boundary layer. Its simplified structure and reduced order provide a manageable framework for the study of fundamental concepts involving the control of linear wavepackets. The objective of this paper is to explore how the sensor-actuator placement interferes in the control problem. This is carried out by evaluating errors of the optimal estimator at positions where control gains are significant. Results show, in quantitative manner, why some choices of sensor/actuator placement are more effective than others for flow control.

1 Introduction

Flow control is a research field that combines the open-loop dynamics of the governing equations given by stability theory, and the input-output approach of control theory, aiming at the manipulation of the system behavior [2]. One of its most prominent objective is the control of instabilities in an airplane wing to delay transition to turbulence and thus reduce the skin friction drag. Several studies regarding control techniques and fundamental concepts have been developed [3, 4], broadening the understanding and the possible exploration areas.

Despite the amount of results available, most studies fix a sensor-actuator structure (placement and shape) and disturbance type and move from this point on. When these parameters are fixed, the specific control problem that is being dealt with does not correspond entirely to the main control objective. As the goal is to achieve the best possible way to control the instabilities, the sensor-actuator structure is in itself a project variable, even considering that in practical applications there is more flexibility to manipulate the placement than the shapes of the sensors and actuators.

Besides the trial-and-error approach of fixing the structure and the disturbance, simulating and comparing the results, a systematic method that helps to treat the sensors and actuators as variables to the problem, explaining in physical terms the reason one given structure provides different results from another, is lacking.

The objective of this work is to provide concepts that help to understand the performance of a specific sensor-actuator placement. This will be done first for the Kuramoto-Sivashinsky equation, a 1D model problem with dynamics similar to transitional boundary layers. The procedure will then be extended for the Blasius boundary layer.

2 Framework

The framework is provided by the Kuramoto-Sivashinsky equation, given by ([1])

$$\frac{\partial v}{\partial t} = -V\frac{\partial v}{\partial x} - \frac{1}{R}\left(P\frac{\partial^2 v}{\partial x^2} + \frac{\partial^4 v}{\partial x^4}\right) + f \qquad (1)$$

linearized around an operating point given by the parameters V, R and P, set as $V = 0.4$, $R = 0.25$

and $P = 0.05$. Here, x and t refer to space and time coordinates, ν is the velocity and f is an external forcing. Supposing an external forcing of the form

$$f(x,t) = b_d(x)d(t) + b_u(x)u(t) \tag{2}$$

The linearized model is represented by the linear time-invariant state-space equation (3).

$$\begin{cases} \dot{q}(t) = Aq(t) + B_u u(t) + B_d d(t) \\ z(t) = C_z q(t) \\ y(t) = C_y q(t) + n(t) \end{cases} \tag{3}$$

where the A matrix includes a discretised differentiation matrix to account for the x-derivatives in (1).

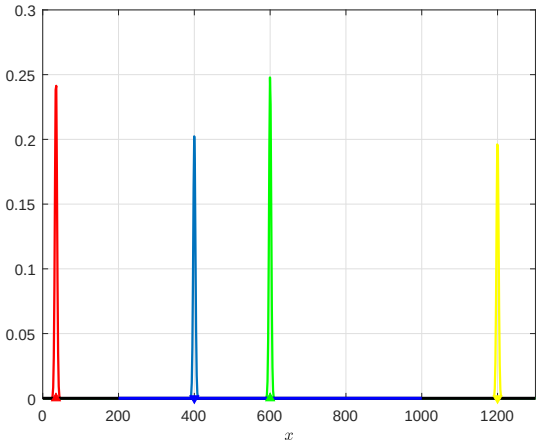

Fig. 1 : An example of the spatial support of the inputs (disturbance B_d(▲) and control B_u(▲)) and outputs (sensor C_y(▼) and objective C_z(▼)).

In this framework, d is an external disturbance, y is the output of the sensor C_y, with measurement noise n, z is the performance variable and B_u the actuator (Fig. 1).

Assuming solutions of the form

$$\nu = \nu' e^{i(\alpha x - \omega t)} \tag{4}$$

where $\alpha \in \mathbb{R}$ and $\omega = \omega_r + i\omega_i \in \mathbb{C}$, the stability analysis of (1) using (4) ($f = 0$) provides the dispersion relation

$$\omega = V\alpha + i\left(\frac{P}{R}\alpha^2 - \frac{1}{R}\alpha^4\right) \tag{5}$$

Its convective and amplifying properties (Fig. 2) make it a good model for the 2D Blasius boundary layer flow. It should be highlighted that the system is globally stable; disturbance growth is seen in a convective frame of reference, but fluctuations eventually leave the computational domain, leading to an overall decay of perturbation energy. Hence, the linear system in (3) is stable. The mentioned convective amplification leads to high amplitude of transfer functions between d and z. Reducing the magnitude of such transfer functions would be the objective of a controller in this framework.

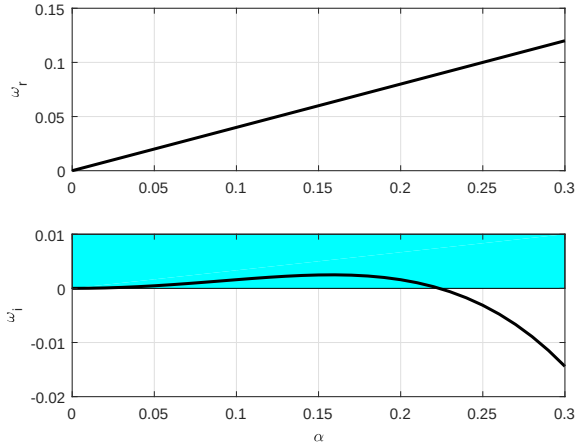

Fig. 2 : The real frequency ω_r and its imaginary part ω_i as a function of the spatial frequency α. Positive values of ω_i characterize unstable waves. Adapted from [1].

3 $\mathcal{H}_2$ Optimization

The objective in the flow control of convective instabilities is to minimize the energy of the linear convective wavepacket in order to delay the transition to turbulence it induces. As the performance variable z in (3) serve as the representation of the disturbance downstream, the objective is to minimize the energy of z.

The control approach that fits this objective is the $\mathcal{H}_2$ optimization. Given the exogenous input w and the control objective z, the controller $H(s)$ internally stabilizes the plant $G(s)$ and optimally

minimize the transfer function $T_{zw}(s)$, *i.e.*, from w to z, according to the $\mathcal{H}_2$ norm (Fig. 3). This is equivalent to minimize the energy of z when w is a stochastic white-noise forcing, as usually is assumed in flow control problems.

Suppose d and n in (3) are white-noise disturbances with spectral densities W and V, respectively. Define the performance z as

$$z(t) = \begin{bmatrix} Q^{\frac{1}{2}}C_z & 0 \\ 0 & R^{\frac{1}{2}} \end{bmatrix} \begin{bmatrix} q(t) \\ u(t) \end{bmatrix} \tag{6}$$

with positive-definite weight matrices Q and R. Despite not being present in (3), the inclusion of the actuation energy in the objective variable z has a precise physical implication. As the actuator has limitations in the input forcing it can provide and it is desirable to minimize the energy spent by the controller, this is in fact a necessary project variable.

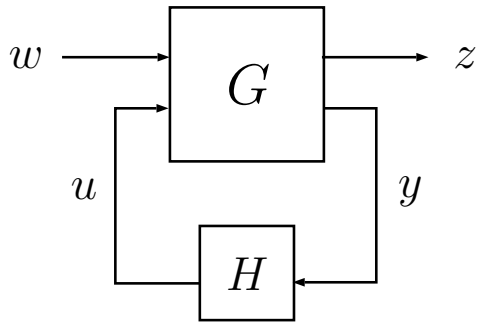

Fig. 3 : General control configuration.

The system's equation (3) is then rewritten as [5]

$$G(s) = \left[\begin{array}{c|cc:c} A & B_d W^{\frac{1}{2}} & 0 & B_u \\ \hline Q^{\frac{1}{2}}C_z & 0 & 0 & 0 \\ 0 & 0 & 0 & R^{\frac{1}{2}} \\ \hdashline C_y & 0 & V^{\frac{1}{2}} & 0 \end{array}\right] \tag{7}$$

where $w(t) = [d(t) \;\; n(t)]'$. The $\mathcal{H}_2$ norm of the transfer function T_{zw} is given by

$$\| T_{zw} \|_2^2 = E\left\{ \lim_{T\to\infty} \frac{1}{T} \int_0^T z^*(t) z(t) dt \right\} \tag{8}$$

This is the LQG problem put in the $\mathcal{H}_2$ optimization framework. The solution to this problem is subject to the separation theorem [6], which states that the optimal control strategy can be separated in two parts: one state estimator which provides the optimal estimation of the system states from the observed outputs, know as the Linear Quadratic Estimator (LQE), and a linear feedback law which gives the control signal as a linear function of the estimated state, known as Linear Quadratic Regulator (LQR) (Fig. 4).

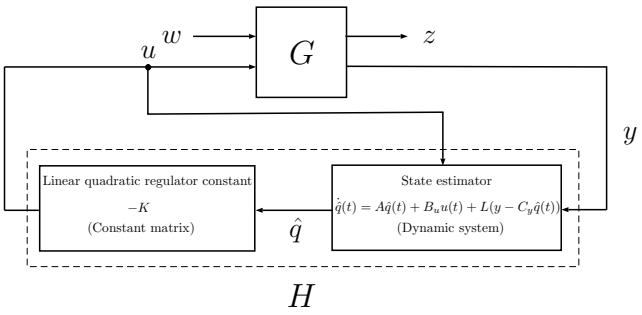

Fig. 4 : LQG control.

4 Full Information

Considering the full information problem, *i.e.*, all the states values are available, the system equation becomes

$$\begin{cases} \dot{q}(t) = Aq(t) + B_u u(t) + B_d d(t) \\ z(t) = C_z q(t) \end{cases} \tag{9}$$

As the goal is to minimize the energy of z, the first question to be answered is if the system is disturbance decoupled by state feedback [7, 8], *i.e.*, if there is a linear map $F : \mathcal{X} \to \mathcal{U}$, where $\mathcal{X}$ is the subspace of admissible states and $\mathcal{U}$ the subspace of admissible inputs, such that

$$T_{zd}(s) = C_z(sI - A - BF)^{-1}B_d = 0 \tag{10}$$

where $T_{zd}(s)$ is the closed-loop transfer function from d to z subjected to the control law $u(t) = Fq(t)$. The expression in (10) can be satisfied if and only if

$$im(B_d) \subset \mathcal{V}^*(ker(C_z)) \tag{11}$$

where $\mathcal{V}^*$ is the largest controlled invariant subspace [7, 8] contained in the subspace $ker(C_z)$.

The control mechanism in convective instability is the generation of a similar wave with opposite phase, *i.e.*, wave cancellation [9]. Disturbance decoupling is then equivalent to the theoretical possibility of the actuator exactly reproduce the incoming wave with opposite phase through state feedback, which would provide the null transfer function in (10).

From this and the intrinsic structural instabililty in operating with subspaces, necessary to the calculation of $\mathcal{V}^*$ through the ISA algorithm [7], the matrix C_z was chosen as shown in Fig. 5, providing equivalent and more reliable results than operating with a single output gaussian C_z as in Fig. 1.

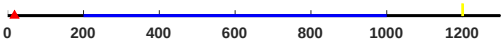

Fig. 5 : Spatial characterization for the ISA algorithm. The red triangle (▲) indicates the disturbance position. In blue is the space available for the actuator placement. In yellow the states expected to be made simultaneously zero, represented by an multiple output C_z.

The condition in (11) is not met for any position available for the actuator (Fig. 5). As the disturbance input is unknown in practice, it is safe to assume perfect control is not achievable even with full state information, once this is not possible when the disturbance is created through a shape similar to the actuator.

In Fig. 6a it is shown that the actuation energy increases as the actuator is moved downstream, as expected given the disturbance is amplified as it moves downstream.

In Fig. 6b it is shown that the LQR performance degrades as the actuator is moved downstream. This result suggests, together with the fact that this system is not disturbance decoupled,

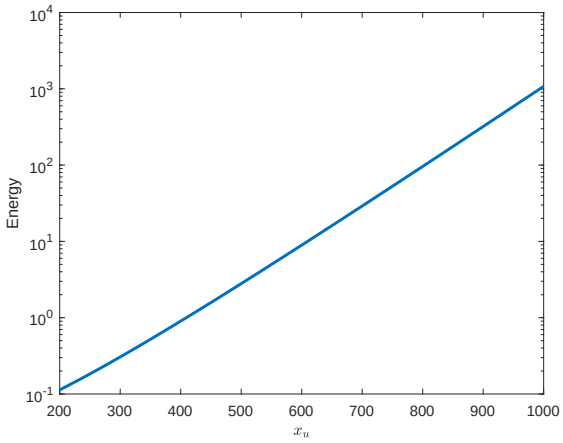

(a) Actuation energy for actuator at position x_u.

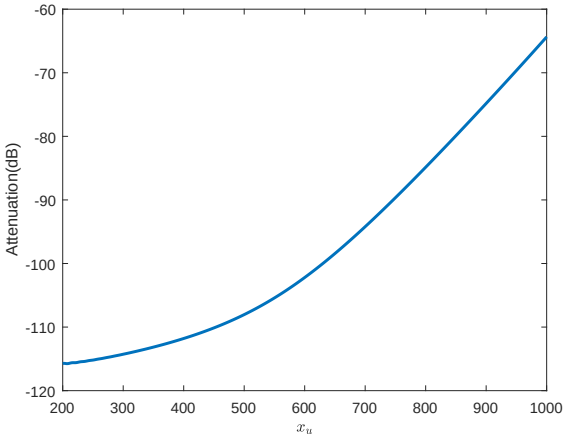

(b) Energy attenuation at z (9) for actuation at position x_u normalized by the uncontrolled energy.

Fig. 6 : LQR control.

that the further the disturbance has developed, the ability of the actuator to reproduce its waveform degrades.

Both results indicates the actuator should be placed as upstream as possible, keeping in mind any unmodelled disturbance that acts in the flow downstream of the actuator will not be controlled.

5 Estimated State

5.1 Motivation

When the states values are not available, as usually is the case, they must be estimated. In Fig. 7 we exemplify the LQE performance by showing the estimated states and associated error for the

system subject to an impulse in d. Results show that the states a particular sensor are able to estimate are those downstream of its position.

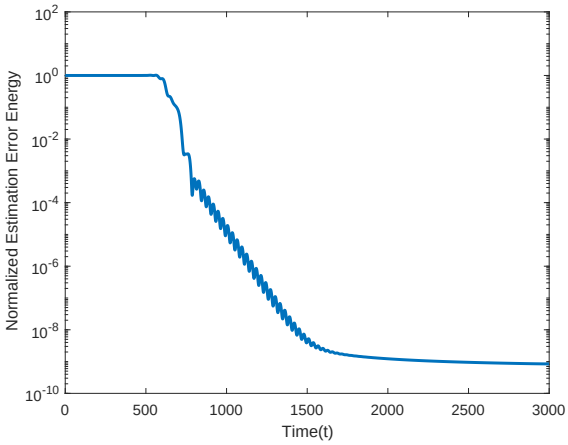

(a) Estimation error energy normalized by the disturbance energy.

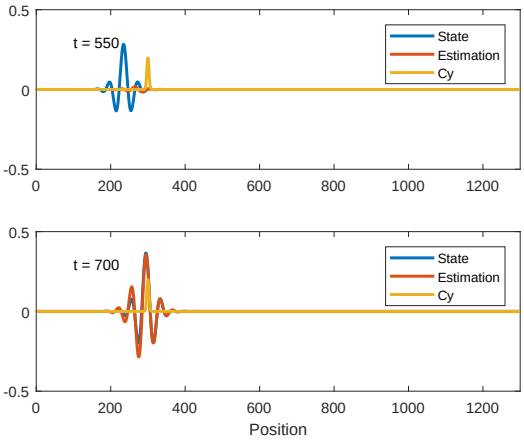

(b) State and estimation for t = 550 and t = 700.

Fig. 7 : LQE for a impulse disturbance for a sensor placed at $x_y = 300$.

For the LQG compensator, the control law is

$$\begin{aligned} u(t) &= -K\hat{q}(t) \\ \hat{q}(t) &= q(t) - e(t) \end{aligned} \tag{12}$$

where K is the linear quadratic regulator (LQR), $q(t)$ the state, $\hat{q}(t)$ the state estimation and $e(t)$ the error in the estimation. When a single control input u is considered, (12) shows that K should be a matrix with dimension equal to the transpose of the state. Hence, the operation $u(t) = -K\hat{q}(t)$ can be seen as the determination of the control by the projection of the estimated state onto the control gains K. Since the state $\hat{q}$ corresponds to fluctuations $v(x,t)$ in the Kuramoto-Sivashinky system, the gains K also have an implicit spatial dependence and can be evaluated to determine which x positions require an accurate estimation of the state. The shape of the gains of the linear quadratic regulator (Fig. 8) implies that a sensor placed downstream to the actuator is not a wise choice, as the controller will use the estimation of states that the estimator cannot properly estimate.

The equation for the closed-loop system with LQG control can be written as

$$\begin{aligned} \dot{q}(t) &= Aq(t) - B_u K\hat{q}(t) + B_d d(t) \\ \dot{q}(t) &= Aq(t) - B_u Kq(t) + B_u Ke(t) + B_d d(t) \end{aligned} \tag{13}$$

where the estimation error satisfiese

$$\dot{e}(t) = (A + LC_y)e(t) + B_d d(t) \tag{14}$$

The estimation error, then, acts as a disturbance that deviates the LQG controlled system behavior from the LQR controlled (full-information) system behavior (Fig. 6b); this can be seen by the additional term $B_u Ke(t)$ in (13) when compared to the full-information control (9). To minimise this deviation, the actuator (which determines K) and the sensor (which determines L) should be placed such that

$$\gamma(x_u, x_y) = \int_0^{+\infty} \| Ke(t) \|_2^2 \, dt \tag{15}$$

is as small as possible.

As shown in Fig. 9, γ achives high values for the actuator upstream to the sensor, and keeps a slowly varying value as the actuator is placed downstream to the sensor. This result, together with the result in Fig. 7, suggests that for high values of γ, $Ke(t) \to Kq(t)$, *i.e.*, the estimator is unable to make any estimation of the states used by the LQR controller, making the system approach the uncontrolled performance (See (13)). For small values of γ, $Ke(t) \to 0$, making the system approach the LQR controlled system performance in Fig. 6.

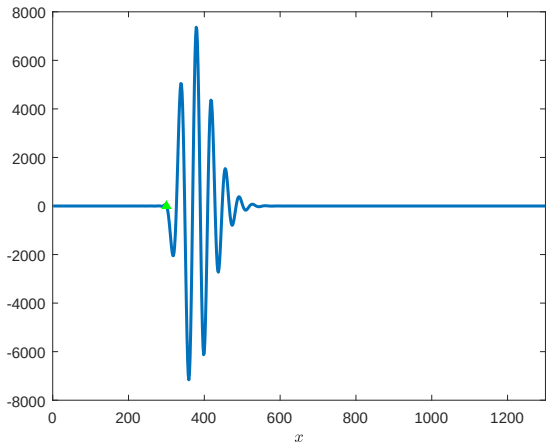

Fig. 8 : Linear quadratic regulator for an actuator at $x_u = 300$(▲).

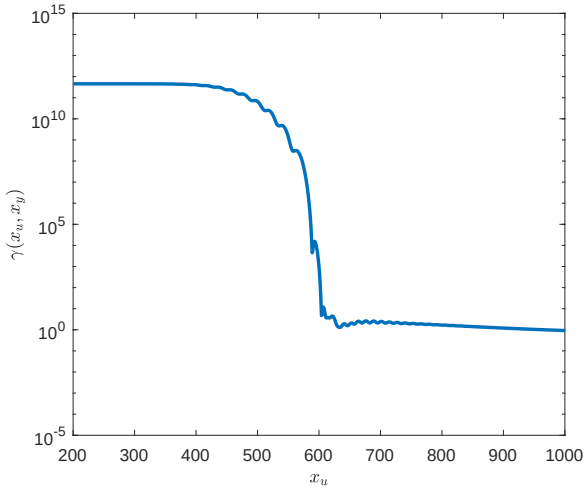

Fig. 9 : γ value for the LQG controlled system for a sensor placed at $x_y = 600$.

Another way to see (15) is representing it as

$$\gamma(x_u, x_y) = \int_0^{+\infty} \| Ke(t) \|_2^2 \, dt = trace(KP_eK^*) \tag{16}$$

where P_e, the covariance of the error, is the solution of the Lyapunov equation

$$(A + LC_y)P_e + P_e(A + LC_y)^* + B_dB_d^* = 0 \tag{17}$$

Performing the singular value decomposition in the matrix P_e

$$P_e = \begin{bmatrix} \cdots & | \phi_{*ev} | & \cdots \end{bmatrix} \begin{bmatrix} \ddots & & \\ & \sigma_{cev} & \\ & & \ddots \end{bmatrix} \begin{bmatrix} \vdots \\ \hline \phi^*_{*ev} \\ \hline \vdots \end{bmatrix} \tag{18}$$

the expression (16) can be rewritten as

$$\gamma(x_u, x_y) = \sum_v \sigma_{cev} < \phi_{ev} | K^* >^2 \tag{19}$$

The value of γ can be regarded as a measure to the extent the modes ϕ_{ve} are projected on the LQR gain K, weighted by the singular values σ_{cev} (Fig. 10). In Fig. 10 (a) we see a case where the gains K and the estimation error modes ϕ_{ev} have completely distinct spatial support; in this case, $\gamma \to 0$ and the LQG performance approaches full-information control. As the actuator is moved upstream (Fig. 10 (b) and (c)) we start to have overlap between the spatial support of K and ϕ_{ev}, until we reach the critical condition shown in Fig. 10 (c), where estimation error is significant precisely at positions where the state should be estimated accurately; in this condition, we expect a poor control performance, close to the open-loop condition.

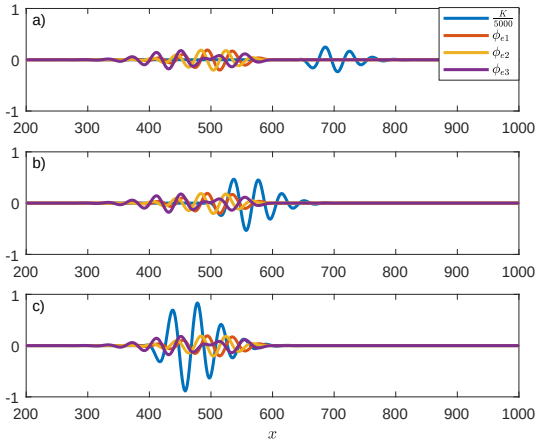

Fig. 10 : Spatial support of the LQR K gain for a) $x_u = 650$, b) $x_u = 500$, c) $x_u = 400$ and the ϕ_e modes for $x_y = 600$ (Fig. 9).

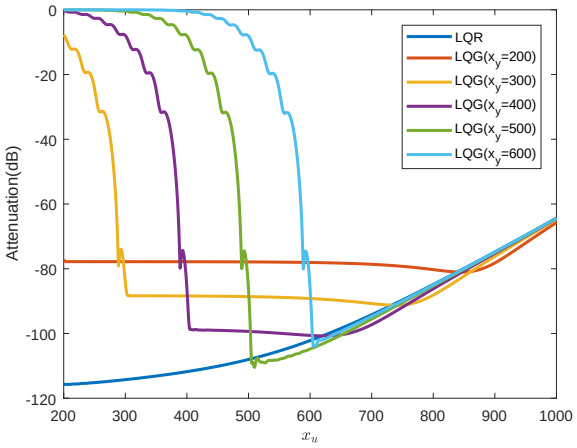

Fig. 11 : Energy attenuation at z normalized by the uncontrolled energy.

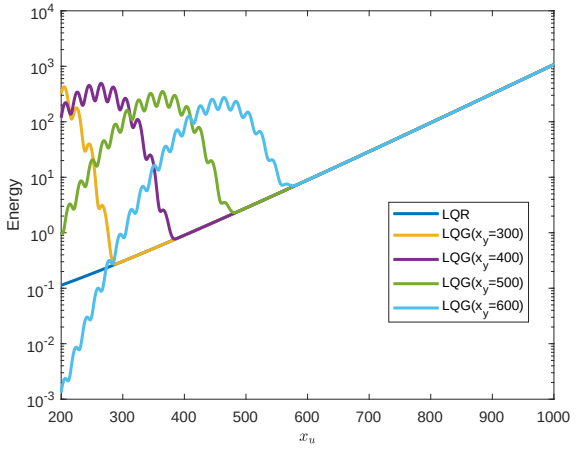

Fig. 12 : LQG actuation energy for actuator at position x_u.

5.2 Control Performance

The performances of various control systems are summarised in Fig. 11. The results indicate as the actuator is placed downstream to the sensor, the performance improves dramatically. As the actuator is moved further downstream, the performance is dominated by the effect of γ, which then remains almost constant until the degradation of the actuator's ability to reproduce the incoming waveform (as decribed in Sec. 4) becomes more prominent and dominates the controlled system performance.

Despite the exponential growth of the actuation energy as the actuator is moved downstream, the performance gain is minimal in the relatively flat portion of the performance curve. This leads to a similar placement rule to the one proposed in Sec. 4: the actuator should be placed downstream of the sensor, upstream enough to reach the relatively flat performance curve (in the γ-dominated zone) or to achieve the best performance (in the actuator's degradation-dominated zone).

The actuation energy for LQG controlled system with the actuator downstream to the sensor is similar to the LQR controlled system actuation energy (Fig. 12), as described in Sec. 5.1.

5.3 γ-dominated Region

The space available for the sensor-actuator placement is divided in two regions: the γ-dominated and the actuator's degradation-dominated regions. The LQR performance curve (Fig. 6a) provides the actuator's degradation effect.

The proposed approach is to describe the estimation error effect through the γ function. It is calculated for the sensor-actuator placements described in the end of Sec. 5.2, *i.e.*, downstream of the sensor, but sufficiently upstream. This distance will be assumed to be $x_u - x_y = 10$. As the actuator's degradation is in its lowest level for the actuator's furthest upstream position ($x_u = 210$), it is assumed that the performance variation is defined by the γ variation. To see this, the γ curve is shifted by

$$\frac{E_{lqr}(x_u = 210)}{E_{ol}} * \gamma \tag{20}$$

where $\frac{E_{lqr}(x_u=210)}{E_{ol}}$ is the LQR controlled system performance for $x_u = 210$. This is the proposed curve representative of the γ effect on the LQG performance(Fig. 13). Here we see that attenuation by control is dictated either by the LQR performance (for a downstream sensor-actuator pair) or by estimation error (for an upstream pair, where the γ effect on performance becomes more

significant).

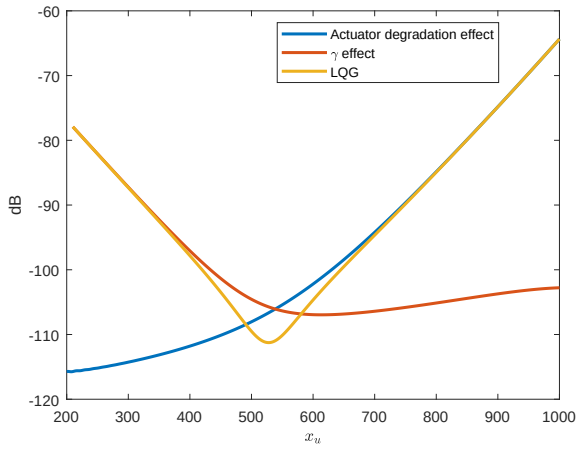

Fig. 13 : Dominated regions and the LQG performance for $x_u - x_y = 10$.

6 Model Reduction Effect

A major limitation faced in flow control is the high order of the systems under study. In this sense, it is not feasable to obtain any of the curves in Fig. 13 directly, once it would be necessary to calculate the full-order optimal state feedback matrix (Fig. 8) and perform the full-order simulation to each point (or a reasonable amount of points).

This limitation imposes the need to work with a reduced order model flow. From this reduced order model a reduced order controller is calculated and applied to the system. Obtaining a reduced order model through balanced truncation [10], the reduced order controller performance is depicted in Fig. 14.

It can be seen that the need for a reduced order controller is an important source of error. Errors due to model reduction are often larger than the those shown in Fig. 13, and, when the order is too low, it dominates the system performance.

7 2D Boundary Layer Example

The simulation of a controlled 2D Blasius boundary layer was carried out with the SIMSON

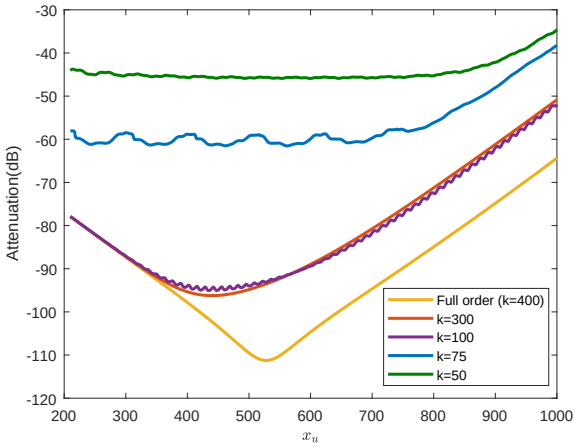

Fig. 14 : LQG controlled system performance with reduced order controllers.

pseudo-spectral solver [11]. The reduced order model was calculated through the eigensystem realisation algorithm (ERA) [12] (Fig. 15).

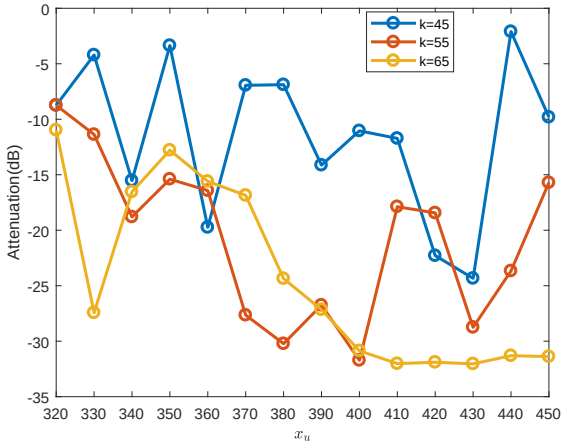

Fig. 15 : 2D Blasius boundary layer controlled with LQG reduced order controllers. The sensor is at the fixed position $x_y = 300$ and the objective at $x_z = 500$.

For the controller with order $k = 65$, the performance resembles what is seen in Fig. 11. The performance oscillates when the actuator is closer to the sensor, and when downstream enough, it reachs a relatively flat performance zone. For lower order controllers, the order reduction error dominates the performance and no

explicit pattern is detectable.

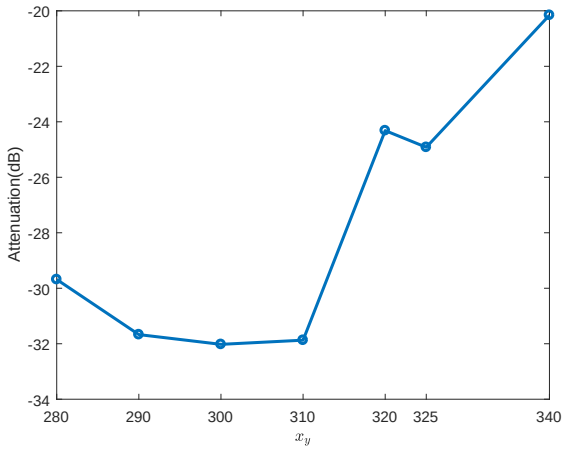

Fig. 16 : 2D Blasius boundary layer controlled with LQG controllers of order $k = 65$. The distance $x_u - x_y = 110$ is fixed and $x_z = 500$.

In Fig. 15, the flat performance zone is achieved when $x_u - x_y \approx 110$. Keeping this distance fixed, the energy attenuation is as shown in Fig. 16. The performance resembles what is shown in Fig. 13. It can be seen that for a boundary layer around 12 dB in performance can be won or lost by changing the positioning of the sensor and actuator, using the same control strategy.

8 Conclusion

The role of the sensor-actuator placement as a project variable cannot be neglected, as implied by the model problem and shown in a boundary layer simulation. An attempt to explain in physical terms the reasons for good and bad performance was presented. Further developments, applying the balanced POD [13] model reduction method, will possibly enable a more clear understanding for boundary-layer control, as the physical interpretation of the reduced state can be retrieved.

References

[1] Fabbiane N, Semeraro O, Bagheri S and Henningson D. *Adaptive and Model-Based Control Theory Applied to Convectively Unstable Flows*, Applied Mechanics Reviews, Vol. 66, 2014.

[2] Bagheri S, Henningson D, Hoepffner J and Schmid P. *Input-Output Analysis and Control Design Applied to a Linear Model of Spatially Developing Flows*, Applied Mechanics Reviews, Vol. 62, 2009.

[3] Bagheri, S and Henningson, D S. *Transition delay using control theory*. Philosophical Transactions of The Royal Society, 2011.

[4] Kim, J and Bewley, T R. *A Linear Systems Approach to Flow Control*. Annual Review of Fluid Mechanics, Volume 39:383-417, January 2007.

[5] Skogestad S, Postlethwaite I. *Multivariable Feedback Control*. 2nd edition, John Wiley & Sons, 2005.

[6] Åström, K J. *Introduction to Stochastic Control Theory*. 1st edition, Academic Press, 1970.

[7] Trentelman, H L, Stoorvogel, A A and Hautaus, M. *Control Theory for Linear Systems*. Springer-Verlag, 2001.

[8] Wonham, W L. *Linear Multivariable Control*. Springer-Verlag, 1985.

[9] Sasaki, K, Morra, P, Fabbiane, N, Cavalieri, A V G, Hanifi, A and Henningson, D S. *On the wave-cancelling nature of boundary layer flow control*. Theoretical and Computational Fluid Dynamics, 2018.

[10] Zhou, K, Doyle, J and Glover, K. *Robust and Optimal Control*. Prentice Hall. 2004.

[11] Chevalier, M, Schlatter, P, Lundbladh, A and Henningson, D. *SIMSON - A Pseudo-Spectral Solver for Incompressible Boundary Layer Flows*. 2007.

[12] Ma, Z, Ahuja, S and Rowley, C W. *Reduced-order models for control of fluids using the eigensystem realization algorithm*. Theoretical and Computational Fluid Dynamics, Volume 25, Issue 1-4, pp 233-247, June 2011.

[13] Rowley, C W. *Model Reduction for Fluids, Using Balanced Proper Orthogonal Decomposition*. International Journal of Bifurcation and Chaos, 2005.

9 Contact Author Email Address

To contact the author mail to: gafreire0@gmail.com

Copyright Statement